Chemistry International 5(4) (2019) 258-268

International Scientific Organization
http://iscientific.org/
Chemistry International
www.bosaljournals.com/chemint/

# Adsorption of Cu(II), Ni(II) and Zn(II) ions by nano kaolinite: Thermodynamics and kinetics studies

**Aisha Muthana Alasadi[1], Fawwaz Izzat Khaili[1] and Akl Mohammad Awwad[2,*]**

[1]Department of Chemistry, College of Science, the University of Jordan, Amman, Jordan
[2]Department of Nanotechnology, Royal Scientific Society, Amman, Jordan
*Corresponding author's E. mail: akl.awwad@yahoo.com

## ARTICLE INFO

**Article type:**
Research article
**Article history:**
Received January 2019
Accepted April 2019
October 2019 Issue
**Keywords:**
Sand deposits
Nano kaolinite
Adsorption
Heavy metals
Thermodynamics
Kinetics

## ABSTRACT

An easy route for preparation emulsion of kaolinite ($Al_2Si_2O_5.4H_2O$) from Sweileh sand deposits, west Amman, Jordan by hydrochloric acid under continuous stirring for 4 h at room temperature was performed and nano kaolinite powder was used as an adsorbent for the removal of Cu(II), Zn(II) and Ni(II) ions. Nano kaolinite was characterized by XRD, FT-IR and SEM techniques. Effect of pH, adsorbent dose, initial metal ion concentration, contact time and temperature on adsorption process was examined. The negative values of $\Delta G^o$ and the positive value of $\Delta H^o$ revealed that the adsorption process was spontaneous and endothermic. The Langmuir isotherm model fitted well to metal ions adsorption data and the adsorption capacity. The kinetic data provided the best correlation of the adsorption with pseudo-second order kinetic model. In view of promising efficiency, the nano kaolinite can be employed for heavy metal ions adsorption.

© 2019 International Scientific Organization: All rights reserved.

**Capsule Summary:** A novel natural adsorbent in nano-scale (nano kaolinite) was used for the first time for the removal of toxic metal ions (Cu(II), Ni(II) and Zn(II)) from aqueous solutions and prepared adsorbent showed promising efficiency for metal ions adsorption, which could possibly be used extended for the adsorption of heavy metals ions from effluents.

**Cite This Article As:** A. M. Alasadi, F. I. Khaili and A. M. Awwad. Adsorption of Cu(II), Ni(II) and Zn(II) ions by nano kaolinite: Thermodynamics and kinetics studies. Chemistry International 5(4) (2019) 258-268. https://doi.org/10.5281/zenodo.2644985

## INTRODUCTION

The Cu(II), Ni(II) and Zn(II) ions are toxic pollutant to the human life and aquatic ecosystem. Metal salts are extensively used in many industrial processes such as electroplating, textile, tanneries, dying and metal finishing industries. These heavy metals are considered high toxic metal, therefore the total limits of these metal ions concentration in water 0.05 mg/L and 1 mg/L in wastewater for use in irrigation (WHO, 2008; USEPA, 2004). Heavy toxic metal ions removal from water and industrial wastewater can be achieved by different treatment processes such as ion exchange (Kuhekar et al. 2014), precipitation method (Minas et al., 2017), coagulation (Verma et al., 2013; Un et al., 2015), reverse osmosis (Tripathi and Dwivedi, 2012), electrochemical reduction–precipitation (Hu et al., 2017), ion flotation (Taseidifar et al., 2017), photocatalytic method (Wahyuni et al., 2015), membrane processes (Abu Qdais and Moussa, 2004; Canet et al., 2003), agricultural waste (Amer et al., 2015), *Ceratonia siliqua* bark (Farhan et al., 2012), rice husk (Asrari et al., 2010), modified loquat bark (Salem et al., 2014), Peanut shells and banana peels (Orhan and Buyukgungor, 1993), palm shell activated carbon (Onundi et al., 2010; Zhang et al., 2017; El-Sadaawy and Abdelwhaab, 2014; Bouhamed et al., 2015), graphene oxide (Sitko et al., 2013), *Ficus carcia* leaves (Farhan et al., 2013), natural materials such as kaolinite clay

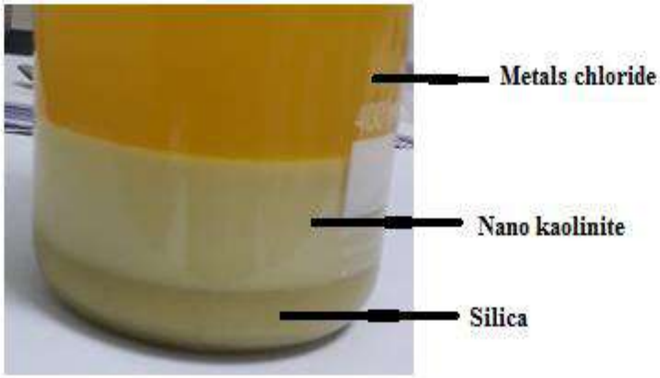

**Fig. 1:** Three layers formed from the reaction of Sweileh sand with hydrochloric acid: Metal chlorides solution, Nano kaolinite and silica

(Kamel et al., 2004; Yavuz et al., 2003), natural clays (Bhattacharyya and Gupta, 2006, Sdiri et al., 2014), natural bentonite (Mellah and Chegrouche, 1997), nano materials and composites (Oang et al., 2015; Choi et al., 2018; Shao-feng et al., 2005; Liu et al., 2014), alginate based nanocomposites (Esmat et al., 2017; Ebadi et al., 2016), natural materials such as sodium bentonite activated clay (Ayari et al., 2007), bentonite and kaolinite (Chai et al., 2007), natural clay (Matlok et al., 2015; Meroufel et al., 2013; Jiang et al., 2010), unmodified and modified kaolinite clay (Al-Essa and Khalili, 2018), kaolinite and metakaolinite (Kounou et al., 2015), polyphosphate modified kaolinite clay (Amer et al., 2010), nano-structured kaolinite (Amer and Awwad, 2017), ligno-cellulose/montmorillonite nanocomposite (Zhang and Wang, 2015), meta-kaolin-based geo-polymer (Cheng et al., 2012) and mechano-chemically treated interstratified montrorillinite/kaolinite (Kumric et al., 2013).

In view of aforementioned facts, present study was focused on preparation of nano kaolinite and adsorption characteristics of nano kaolinite prepared from Sweileh sand deposits, west Amman, Jordan for removal of Cu(II), Ni(II), and Zn(II) ions from aqueous solution in batch process was evaluated along with thermodynamics, equilibrium and kinetics studies.

## MATERIAL AND METHODS

### Chemicals and reagents

Copper sulfate pentahydrate ($CuSO_4$. $5H_2O$), anhydrous zinc acetate (Zn $(CH_3COO)_2$ and nickel sulfate hexahydrate ($NiSO_4$. $6H_2O$), with purity ≥ 98.0%, hydrochloric acid (37%, ACS reagent) and sodium hydroxide (NaOH, 99%) were obtained from Sigma-Aldrich. Sand was collected from Sweileh sand deposits, west, Amman, Jordan. Distilled and deionized water were used in all our experimental work.

### Preparation of nano kaolinite

Sand was collected from Sweileh sand deposits, west Amman, Jordan. Samples were dried in an oven at 80 $^0$C for 4 h. Afterwards, different samples of sand were treated with hydrochloric acid (37%) under continuous stirring at ambient temperature (27$^o$C) for 4-6 h and left over night. Three layers were formed, the upper layer, a brown-yellow composed mainly from metal chlorides ($MCl_2$), the medium layer is composed from emulsion of kaolinite ($Al_2Si_2O_5.4H_2O$) and the third layer (bottom layer) is composed from pure silica ($SiO_2$) (Fig. 1). By decantation and washing with de-ionized water on Whatman filter paper No. 1. Nano kaolinite was obtained as white particles on filter paper and metal chlorides as yellow-brown solution. It was found that Sweileh sand deposits composed mainly from 80-84% pure quartz, 16-18% kaolin clay and 4-8% metal salts.

### Characterization

X-Ray diffraction (XRD) pattern of Nano kaolinite prepared from sand deposits was recorded using XRD-6000 (Schimadzu, Japan) over a wide range of Bragg angles ($10^o \leq 2\theta \leq 80$). Fourier transmission infrared spectroscopy (FT-IR, IR Prestige, and Shimadzu, Japan) was used to identify the chemical functional groups of the prepared Nano kaolinite. Scanning electron microscopy for morphology study was Quanta FEI 450 SEM machine.

The metal ions concentration in solution before and after equilibrium was determined using a sequential plasma emission spectrometer (ICPS-7510, Shimadizu). The pH of the solutions was measured with a WTW pH meter using a combined glass electrode. The specific areas of Nano kaolinite were estimated by a surface analyzer (Quanta chromosorb) and BET method.

### Adsorption procedure

Stock solutions of Cu(II), Ni(II) and Zn(II) ions solutions (1000mg/L) were prepared by dissolving appropriate determined amounts of copper sulfate pentahydrate, nickel sulfate hexahydrate and anhydrous zinc acetate in 1000 ml de-ionized water. Different concentrations from metal ions ranging from 10-120 mg/L were prepared from the stock solutions by dilution. In all experimental work, an accurately weighed quantity of nano kaolinite was added to 100mL of aqueous solution taken in a 250 mL conical flask and the mixture was agitated in a rotary shaker. Analyses of the samples in this research work were done after filtration process using Whitman 42 filter paper. The obtained results were the average of three repeated experiments. The data obtained were used to calculate the percent removal (%R) and equilibrium capacity ($q_e$) of Cu(II), Ni(II) and Zn(II) ions using relations shown in Eq. 1-2, respectively.

$$\text{Cr(VI) removal (\%)} = \frac{C_o - C_e}{C_o} \, x \, 100 \qquad (1)$$

$$q_e = \frac{C_o - C_e}{w} \, x \, V \qquad (2)$$

Where, $C_o$ and $C_e$ are the initial and equilibrium concentrations of metal ions (mg/L), V is the volume of the solution (L) and W is the weight (g) of nano kaolinite adsorbent.

### Isotherm modeling

Langmuir model assumes monolayer adsorption onto a surface (Langmuir, 1918) (Eq. 3).

$$\frac{C_e}{q_e} = \frac{C_e}{q_{max}} + \frac{1}{k_l q_{max}} \qquad (3)$$

Where, $C_e$ is the equilibrium concentration of metal ions in the aqueous phase (mg/L), $k_L$ is the Langmuir adsorption constant, and $q_e$ and $q_{max}$ are the amount of adsorption of metal ions at equilibrium and maximum adsorption capacity on the surface of adsorbent (mg/g), respectively. Freundlich isotherm model is describing the adsorption process. This model applies to adsorption on heterogeneous surfaces with the interaction between adsorbed molecules. This isotherm is an empirical equation and can be employed to describe heterogeneous systems and is expressed as follows in linear form (Freundlich and Hallen, 1939) (Eq. 4).

$$\ln q_e = \ln k_F + \frac{1}{n} \ln C_e \qquad (4)$$

Where, $K_F$ is the Freundlich constant, 1/n is the heterogeneity factor and n (g/L) is a measure of the deviation from linearity of adsorption.

### Kinetic studies

Kinetic models have been proposed to determine the mechanism of the adsorption process, which provide useful data to improve the efficiency of the adsorption and feasibility of process scale-up. In the present study, the mechanism of the adsorption process was studied the experimental data using pseudo-first–order and pseudo-second–order kinetics models (Ho, 2006, Zhan et al., 2018) (Eq. 5-6).

$$\ln(q_e - q_t) = \ln q_e - k_1 t \qquad (5)$$

$$\frac{t}{q_t} = \frac{1}{k q_e^2} + \frac{1}{q_e} \qquad (6)$$

Where, $q_e$ and $q_t$ are the adsorption capacity at equilibrium and time (t) respectively. $K_1$ is the rate constant of the pseudo-first-order adsorption. k is rate constant of the pseudo-second-order adsorption.

### Thermodynamic studies

Adsorption of Cu(II), Ni(II) and Zn (II) ions by the prepared nano kaolinite was studied from thermodynamic point of view to ascertain the nature of adsorption process under the condition of the current study. Thermodynamic parameters, Gibbs free energy ($\Delta G^o$), enthalpy ($\Delta H^o$), and entropy change ($\Delta S^o$), were determined following Eq. 7-9.

$$K_D = \frac{C_a}{C_e} \qquad (7)$$

$$\Delta G^o = -RT \ln K_D \qquad (8)$$

$$\ln K_D = \frac{\Delta S^o}{R} - \frac{\Delta H^o}{RT} \qquad (9)$$

Where, $K_D$ is the distribution coefficient for the adsorption, $\Delta S^o$, $\Delta H^o$, and $\Delta G^o$ are the changes of entropy, enthalpy, and the Gibbs energy. T (K) is the temperature, and R (8.314 J/mol K) is the gas constant. The values of $\Delta H^o$ and $\Delta S^o$ were determined from the slopes and intercepts of the plots of ln $K_D$ versus 1/T.

## RESULTS AND DISCUSSION

### Characterization of nano kaolinite

X-ray diffraction spectrum, Fig. 2 showed that highly pure nano kaolinite with diffraction intensities of kaolinite clay standard (JCPDS-No. 80-2186). Particle of the nano kaolinite was calculated by Debye-Scherer relation (Eq. 10).

$$D = K\lambda/\beta\cos\theta \qquad (10)$$

Where, D is the crystallite size of copper hydroxide nanoparticles, λ represents wavelength of x-ray source 0.1541 nm) used in XRD, β is the full width at half maximum of the diffraction peak, K is the Scherer constant with value from 0.9 to 1 and θ is the Bragg angle. The average size determined was found to be 20nm. The FT-IR spectrum of the prepared nano kaolinite, Fig. 3 showed the hydroxyl stretching vibration bands at 3692 $cm^{-1}$, which corresponds to the inner surface –OH stretching vibration of kaolinite. Band at 3622 $cm^{-1}$ belongs to the stretching vibration of the outer-surface hydroxyl groups, indicating the presence of kaolinite in raw kaolin clay. The bands at 1119, 1041, 995, 910, 799 and 694 $cm^{-1}$ indicated to Si-O bending and stretching vibrations. Absorption band at 910 $cm^{-1}$ corresponds to the Al-O bending vibration. Bands at 536 and 470, 428 $cm^{-1}$ represent to Al-O-Si skeletal vibration. These results indicated that the hydrogen bonding between the layers of raw kaolin and formation of new hydrogen bonding between the inner –surface hydroxyl groups and S=O groups. The obtained results indicated that HCl removed all associated metal oxides in raw Sweileh sand and changed the structure to nano-platelets kaolinite. Scanning electron microscopy (SEM) analysis of nano kaolinite prepared from Sweileh sand deposits has an average diameter 10-120 nm and with average thickness 18 nm. The nano kaolinite consisted of particles with typical platelets shapes (Fig. 4).

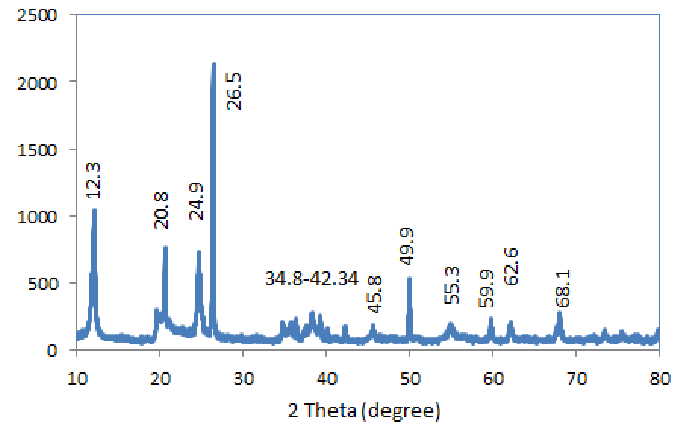

**Fig. 2:** XRD of nano kaolinite extracted from Sweileh sand

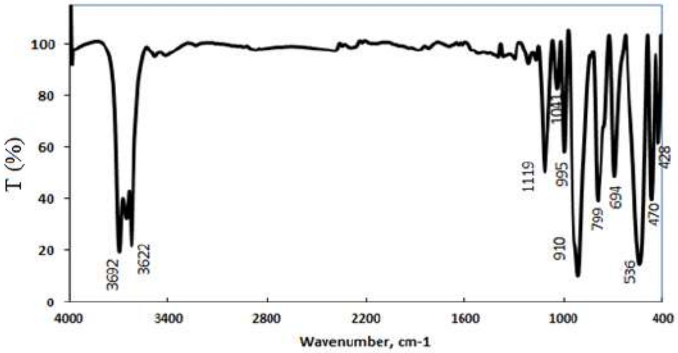

**Fig. 3:** FT-IR of the prepared nano kaolinite from Sweileh sand deposits

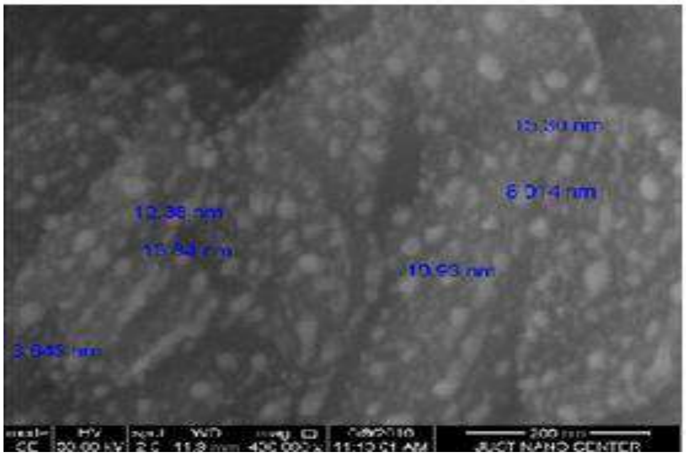

**Fig. 4:** SEM of the prepared nano kaolinite from Sweileh sand deposits

Increasing the time of reaction of sand deposits to 6 h with hydrochloric acid under vigorous stirring at ambient temperature gave nano platelets kaolinite with smaller particle size diameter ranging 3-20 nm. The average size of platelets nano kaolinite obtained was ~10 nm.

### Effect of the initial pH

The effect of pH solutions on the adsorption percent removal of metals onto the nano kaolinite is shown in Fig. 5. The removal percent (%R) of Cu(II), Ni(II) and Zn(II) ions increases sharply with increasing pH from 1.0 to 6.0 and then decreases to reach pH 8.0. The maximum percent removal was observed around pH 5.5-6 at all temperatures.

### Effect of contact time and temperature

The effect of contact time on the adsorption of Cu(II), Ni(II) and Zn(II) ions onto nano kaolinite is illustrated in Fig. 6. It can be seen that the removal percent (R%) of Cu(II), Ni(II) and Zn(II) increases with contact time until equilibrium is attained between the amount of metal ions and nano kaolinite and the remaining metals in solution. The removal percent increases with contact time from (0 to 60 min) and then becomes almost constant up to the end of the experiment. It can be concluded that the binding of metal ions with nano kaolinite is high at initial stages and becomes almost constant after an optimum contact time of 120 min. This indicated that the adsorption process is endothermic in nature. The metals removal percent versus time curves are smooth and continuous leading to saturation, suggesting possible monolayer coverage of Cu(II), Ni(II) and Zn(II) ions on the surface of the nano kaolinite.

### Effect of adsorbent dose

The effect of adsorbent dose of nano kaolinite on the Cu(II), Ni(II) and Zn (II) ions removal percent increased very rapidly with an increase in dosage of nano kaolinite from (0.1 to 1.0 g/L) and a marginal increase was observed on further increase in the adsorbent dose. At an adsorbent dose of 1.0 g/L. the increase in efficiency of metals removal may be attributed to the fact that, with an increase in the adsorbent dose, more adsorbent surface or more adsorption sites were available for the metal ions to be adsorbed.

### Adsorption Isotherms

Isotherms models were studied for characterization of the adsorption process such as Langmuir and Freundlich isotherms, which provide information on the capacity of sorbent. The Langmuir model been empirically most often used, contained the two parameters $q_m$ and $K_L$, which reflect the two important characteristics of the sorption systems. Equilibrium capacity $q_e$ was calculated for each metal concentration by plotting $C_e$ against $C_e/q_e$. Fig. 7 showed a straight line was fitted in the data. Correlation factor $R^2$ for, Cu (II), Ni (II), and Zn (II) indicated that sorption followed Langmuir model. Values of Langmuir constants $q_m$ and $K_L$ were calculated from slope and intercept of line. The Langmuir plots Cu (II), Ni (II) and Zn (II) isothermal adsorption data for nano kaolinite adsorbent at 30°C are shown in Fig. 7.

**Table 1:** Langmuir and Freundlich constants of Cu (II), Ni (II) and Zn (II) ions onto nano kaolinite

| | Langmuir model | | | Freundlich model | | |
|---|---|---|---|---|---|---|
| Metal ion | $q_{max}$ (mg/g) | $K_L$ (L/g) | $R^2$ | n (g/L) | $K_F$ (mg/g) | $R^2$ |
| Cu (II) | 125 | 0.022 | 0.9999 | 1.269 | 0.155 | 0.9801 |
| Ni (II) | 111 | 0.021 | 0.9999 | 1.193 | 0.167 | 0.9889 |
| Zn (II) | 100 | 0.019 | 0.9999 | 1.069 | 0.928 | 0.9839 |

**Table 2:** Thermodynamic Parameters of Nano kaolinite for Cu (II), Ni (II)and Zn (II) ions adsorption

| T (K) | ln $K_D$ | $\Delta G^o$ (kJ/mol) | $\Delta H^o$ (kJ/mol) | $\Delta S^o$ (J/K.mol) |
|---|---|---|---|---|
| | Cu (II) | | | |
| 293 | 1.65 | -4.02 | 15.71 | 67.33 |
| 303 | 1.86 | -4.84 | | |
| 313 | 2.07 | -5.36 | | |
| | Ni (II) | | | |
| 293 | 1.17 | -2.85 | 21.49 | 83.1 |
| 303 | 1.47 | -3.71 | | |
| 313 | 1.73 | -4.5 | | |
| | Zn (II) | | | |
| 293 | 1.09 | -2.66 | 22.17 | 84.8 |
| 303 | 1.41 | -3.55 | | |
| 313 | 1.68 | -4.37 | | |

**Table 3:** Adsorption capacity (mg/g) of various adsorbents and present study

| Adsorbent | Cu (II) | Ni (II) | Zn (II) | References |
|---|---|---|---|---|
| Nano-structured kaolinite | 45.87 | | 52.63 | Amer and Awwad (2017) |
| Cation exchange resin | 164 | 109 | 105 | Revathi et al. (2012) |
| Alignate modified with polyethyleneimine | 177.1 | | 110.2 | Zhan et al. (2018) |
| Graphene oxide | 294 | | 345 | Sitko et al. (2013) |
| Polyphosphate-modified kaolin | | | 27.78 | Amer et al. (2010) |
| Natural clay | 44.84 | | 80.64 | Veli and Alyuz (2007) |
| Kaolinite | 10.787 | 1.669 | | Yavuz et al. (2003) |
| Activated carbon | 18.68 | 16.12 | 12.19 | El-Sadaawy and Abdelwahab (2014) |
| Nano kaolinite | 125 | 111 | 100 | This work |

For all metal ions, $R^2$ values > 0.9999 which clearly suggests the applicability of Langmuir adsorption model. The calculated constants $q_m$ and $K_L$ together with correlation coefficients ($R^2$) are given in Table 1. The values of $q_m$ increased with the rise of temperatures, indicating the sorption processes are endothermic in nature. The constant, $K_L$ is related to the affinity between the adsorbent and adsorbate. The values of $K_L$ increased slightly with increasing temperature. Low values of parameter $K_L$ indicate that nano kaolinite have high affinity for Cu (II), Ni (II), and Zn (II) ions.

Freundlich isotherm model applies to adsorption on heterogeneous surfaces with the interaction between adsorbed molecules and the application of the Freundlich equation, also suggests that sorption energy exponentially decreases on completion of the sorption centers of an adsorbent. Equilibrium constants were determined from the plot of $\ln q_e$ versus $\ln C_e$ (Fig. 8). The n value indicates the degree of non-linearity between solution concentration and adsorption as follows: if n = 1, then adsorption is linear; if n<1, then adsorption is a chemical process; if n>1, then adsorption is a physical process.

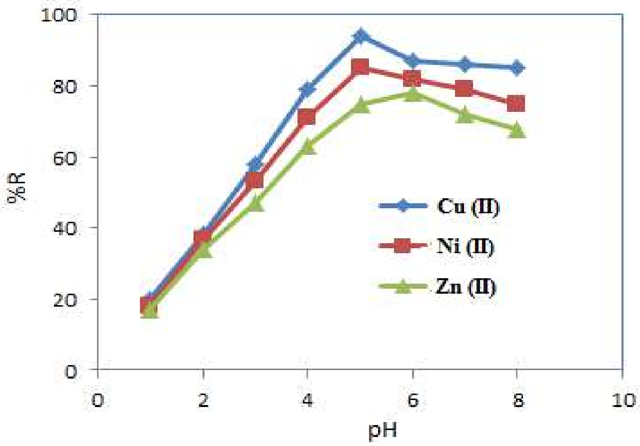

**Fig. 5:** Effect of pH solution on the percent removal of metal ions by nano kaolinite (T =303 K; 40 mg/L; pH = 5.5 - 6).

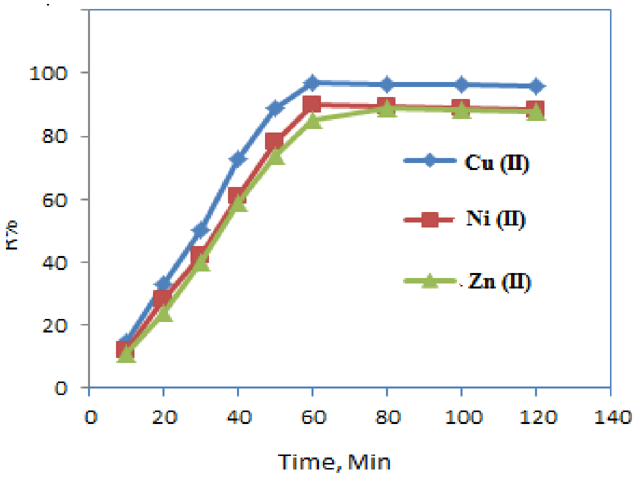

**Fig. 6:** Effect of contact time (min) on the percent removal of Cu(II), Ni(II) and Zn(II) ions by nano kaolinite; Initial metals concentration 40mg/L at 30°C.

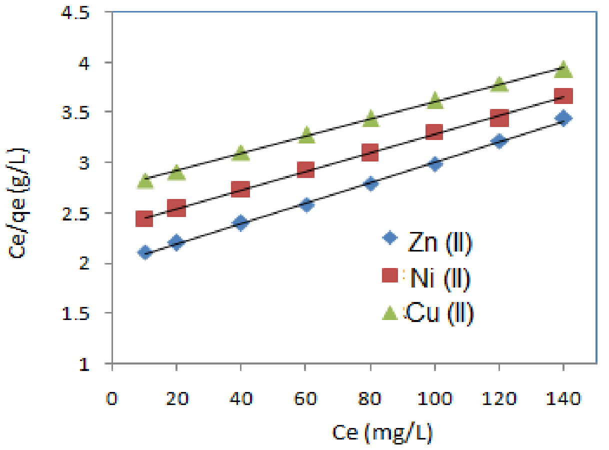

**Fig. 7:** Langmuir isotherm for Cu (II), Ni (II), and Zn (II) ions onto nano kaolinite.

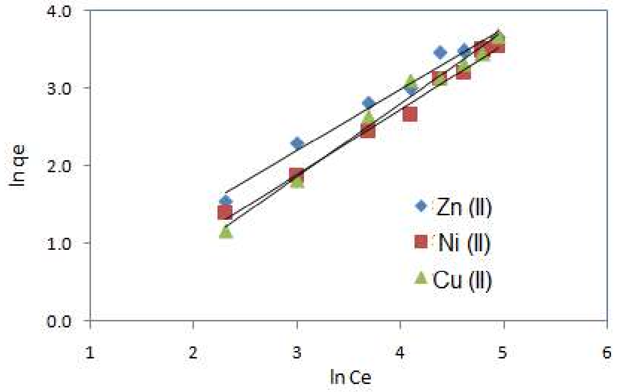

**Fig. 8:** Freundlich isotherms for Ni (II), Zn (II) and Cu (II) ions onto nano kaolinite

The n value in Freundlich equation was found at 30 °C to be 2.57, 2.11 and 1.98 for Cu (II), Zn (II) and Zn (II) ions, respectively (Table 2). Since n lie between 1 and 10, this indicates the physical adsorption of metal ions onto nano kaolinite. The values of regression coefficients $R^2$ are regarded as a measure of goodness of fit of the experimental data to the isotherm models.

### Thermodynamic parameters

The thermodynamic behavior of the adsorption of Cu(II), Ni(II), and Zn (II) ions onto nano kaolinite obtained from Sweileh sand deposits. Thermodynamic parameters including the change in free energy ($\Delta G^o$), enthalpy ($\Delta H^o$) and entropy ($\Delta S^o$) were calculated. According to thermodynamics, the Gibb's free energy change is also related to the enthalpy change ($\Delta H^o$) and entropy change ($\Delta S^o$) at constant temperature by the Gibbs–Helmholtz (Eq. 11).

$$\Delta G^o = \Delta H^o - T\Delta S^o \quad (11)$$

The values of enthalpy change ($\Delta H^o$) and entropy change ($\Delta S^o$) were calculated from the slope and intercept of the plot of ln $K_D$ vs. 1/T, Fig. 9. The calculated values of thermodynamic parameters $\Delta G^o$, $\Delta H^o$ and $\Delta S^o$ for the adsorption of Cu (II), Ni (II), and Zn(II) ions onto nano kaolinite are reported in Table 2. A negative value of the free energy ($\Delta G^o$) indicated the spontaneous nature of the adsorption process. It was also noted that the change in free energy, increases with rise in temperature. This could be possibly because of activation of more sites on the surface of nano kaolinite with increase in temperature or that the energy of adsorption sites has an exponential distribution and a higher temperature enables the energy barrier of adsorption to be overcome. For physical adsorption, the free energy change ($\Delta G^o$) ranges from (-20 to 0) kJ/mol and for chemical adsorption it ranges between (-80 and -400) kJ/mol.

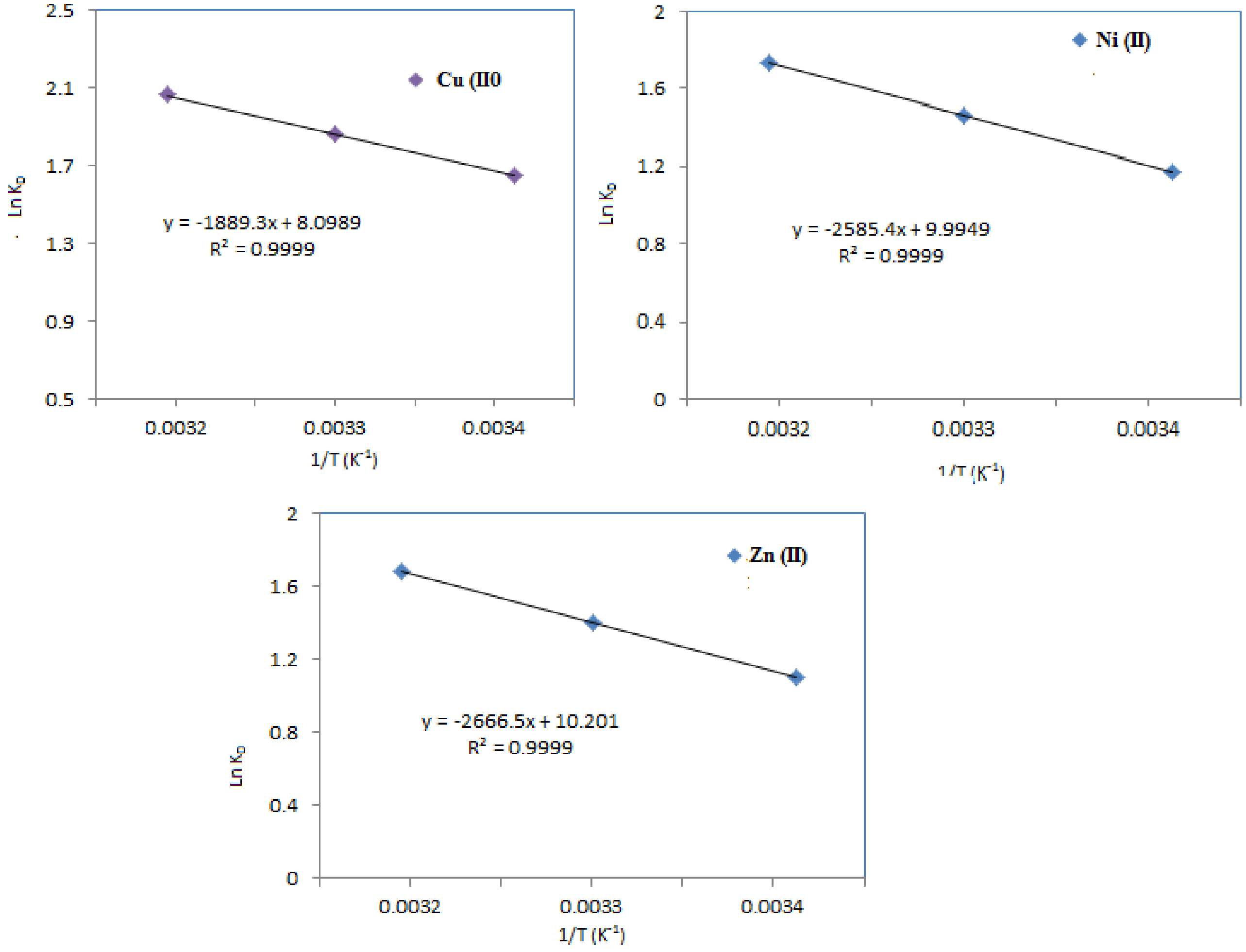

**Fig. 9:** ln $K_D$ vs 1/T for the adsorption of Cu (II), Ni (II) and Zn (II) ions.

The ΔG° for Cu (II), Ni(II) and Zn (II) adsorption onto nano kaolinite was in the range of (2.66 to -5.36) kJ/ mol and so the adsorption was predominantly physical adsorption. A positive value of ΔS° as 67.33–84.80 J/mol K showed increased randomness at solid solution interface during the adsorption of Cu (II), Ni (II) and Zn (II) ions onto nano kaolinite.

## Adsorption kinetics

Pseudo-first-order and pseudo-second-order were fit to experimental data to examine the adsorption kinetics of Cu (II), Ni (II), and Zn (II) ions uptake onto nano kaolinite. The equation applicable to experimental results generally differs from a true first-order equation in two ways: the parameter $k_1(q_e\text{-}q_t)$ does not represent the number of available sites; and the parameter ln $q_e$ is an adjustable parameter which is often not found equal to the intercept of a plot of ln $(q_e\text{-}q_t)$ against t, whereas in a true first-order sorption reaction log $q_e$ should be equal to the intercept of $\ln(q_e\text{-}q_t)$ against t. To fit the equation to experimental data, the equilibrium sorption capacity, $q_e$ must be known. In many cases is unknown and as chemisorption tends to become un measurably slow, the amount sorbed is still significantly smaller than the equilibrium amount. In most cases in the literature, the pseudo-first-order equation of Lagergren does not fit well for the whole range of contact time and is generally applicable over the initial 20–60 min of the sorption process. Furthermore, one has to find some means of extrapolating the experimental data to t = α on treating $q_e$ as an adjustable parameter to be determined by trial and error. For this reason, it is therefore necessary to use trial and error to obtain the equilibrium sorption capacity, to analyze the pseudo-first-order model kinetics. The pseudo-first-order rate constant can be obtained from the slope of plot between log $(q_e\text{-}q_t)$ against time (t) (Fig. 10). The calculated values and their corresponding linear regression correlation coefficient values are listed in Table

5. $R^2$ was found to be 0.926, which shows that this model cannot be applied to predict the adsorption kinetics If pseudo-second-order kinetics is applicable, the plot of $t/q_t$ versus t should give a linear relationship, from which qe and $k_2$ can be determined from the slope and intercept of the plot, Fig. 11. The pseudo-second-order rate constant $k_2$, the calculated qe value and the corresponding linear regression correlation coefficient value are given in Table 6. At all initial metal concentrations, the linear regression correlation coefficient $R^2$ values were higher. This confirms the adsorption data are well represented by pseudo-second-order kinetics.

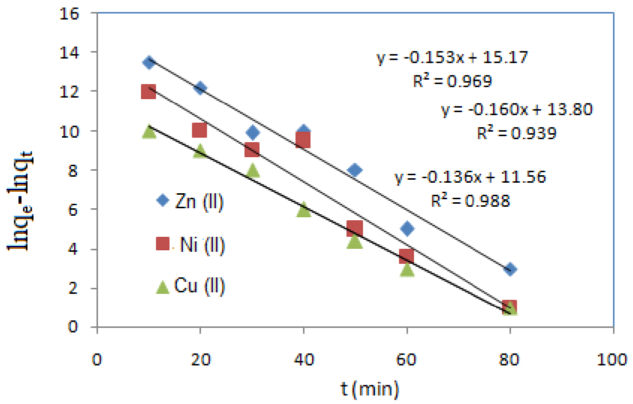

**Fig. 10:** Pseudo-first-order kinetics for metal ions onto nano kaolinite

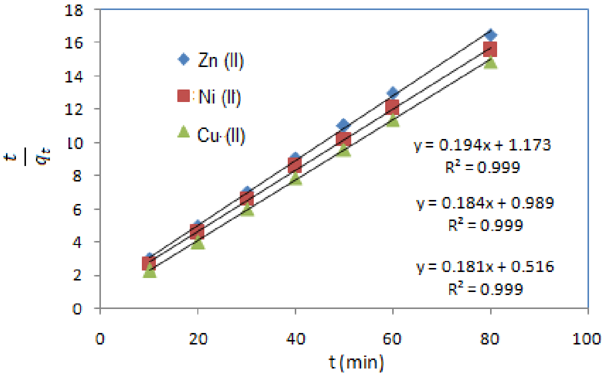

**Fig. 11**: Pseudo-second-order kinetics for metal ions onto nano kaolinite

### Comparison of nano kaolinite with other adsorbents

A comparative of the maximum adsorption capacity, $q_{max}$ of nano kaolinite with some of other adsorbents reported in literature, Table 3. Differences in $q_{max}$ are due to the nature, purity and properties of each adsorbent such as surface area and the main functional groups in the structure of the adsorbents. A comparison with other adsorbents indicated a high metal ion adsorption capacity of nano kaolinite extracted and prepared from deposits of Sweileh sand, west Amman, Jordan. Findings revealed that nano kaolinite offered promising adsorption efficiency versus various other adsorbents reported for metal ions adsorption and nano kaolinite could possibly be used for the adsorption of heavy metal ions from industrial effluents (Bulgariu et al., 2019; Chen et al., 2019; Gaikwad et al., 2010; Godiya et al., 2019a; Godiya et al., 2019b; Ibrahim and Fakhre, 2019; Jiang et al., 2019; Kausar et al., 2018a; Kausar et al., 2018b; Khera et al., 2019; Liang et al., 2013; Mousavi et al., 2019; Nadeem et al., 2016; Sandoval et al., 2019; Zafar et al., 2018; Zhao et al., 2019).

## CONCLUSIONS

The results in this research paper demonstrate that nano kaolinite obtained from Sweileh sand deposits is an effective adsorbent and can be successfully used as an adsorbing agent for the removal of Ni(II), Zn(II) and Cu(II) ions from aqueous solutions. The thermodynamic parameters, $\Delta H^o$, $\Delta S^o$, and $\Delta G^o$ values of metal ions adsorption onto nano kaolinite showed the endothermic heat of adsorption, favored at high temperatures. The positive values of $\Delta S^o$ revealed an increase in randomness of the solid-solution interface during the adsorption of metal ions. Regression coefficient $R^2$ were found to be more than 0.999 revealing the best fit for the adsorption data by the Langmuir isotherm model over the Freundlich isotherm model. The kinetic data provided the best correlation of the adsorption of Cu (II), Ni (II) and Zn (II) onto nano kaolinite obtained from Sweileh sand deposits by pseudo-second order equation. The nano kaolinite compared favorably with different kaolin clay adsorbents.

## ACKNOWLEDGEMENTS

The authors are thankful to the Royal Scientific Society and the University of Jordan, Amman, Jordan for giving all facilities to carry out this research work.

## REFERENCES

Abu Qdais, H., Moussa, H., 2004. Removal of heavy metals from wastewater by membrane processes: a comparative study, Desalination 164, 105-110.

Al-Essa, K., Khalili, F., 2018. Heavy metals adsorption from aqueous solutions onto unmodified and modified Jordanian kaolinite clay: Batch and column techniques, American Journal of Applied Chemistry 6, 25-34.

Amer, M. W., Khalili F. I., Awwad A.M., 2010. Adsorption of lead, zinc and cadmium ions on polyphosphate-modified kaolinite clay. Journal of Environmental Chemistry and Ecotoxicology 2, 1-8.

Amer, M., Awwad, A.M., 2017. Removal of Zn(II), Cd(II) and Cu(II) Ions from aqueous solution by nano-structured kaolinite. Asian Journal of Chemistry 29, 965-969.

Amer, M.W., Ahmad, R.A., Awwad, A.M., 2015. Biosorption of Cu(II), Ni(II), Zn(II) and Pb(II) ions from aqueous solution by *Sophora japonica* pods powder, International Journal of Industrial Chemistry 6, 67–75.

Asrari, E., Hossein, T.A., Mahnoosh, H., 2010. Removal of Zn(II) and Pb(II) ions using rice husk in food industrial waste water. Journal of Applied Sciences and Environmental Management 14, 159–162.

Ayari, F., Srasra, E., Trabelsi-ayadi, M., 2007. Removal of lead, zinc and nickel using sodium bentonite activated clay. Asian Journal of Chemistry 19, 3325-3339.

Bhattacharyya, K.G., Gupta, S.S., 2006. Adsorption of chromium(VI) from water by clays. Industrial & Engineering Chemistry Research 45, 7232–7240.

Bouhamed, F., Eloucar, Z., Bouzid, J., Ouddane, B., 2015. Multi-component adsorption of copper, nickel and zinc from aqueous solutions onto activated carbon prepared from date stones. Environmental Science and Pollution Research 23, 15801-15806.

Bulgariu, L., Escudero, L.B., Bello, O.S., Iqbal, M., Nisar, J., Adegoke, K.A., Alakhras, F., Kornaros, M., Anastopoulos, I., 2019. The utilization of leaf-based adsorbents for dyes removal: A review. Journal of Molecular Liquids 276, 728-747.

Canet, L., Ilpide, M., Seat, P., 2003. Efficient facilitated transport of lead, cadmium, zinc and silver across a flat sheet-supported liquid membrane mediated by lasalocid A. Separation Science and Technology 37, 1851–1860.

Chai, W., Huang, Y., Su, S., Han, G., Liu, J., Cao, Y., 2017. Adsorption behavior of Zn (II) onto natural minerals in wastewater. A comparative study of bentonite and kaolinite. Physicochemical Problems of Mineral Processing 53, 264-278.

Chen, J., Zhu, J., Wang, N., Feng, J., Yan, W., 2019. Hydrophilic polythiophene/SiO2 composite for adsorption engineering: Green synthesis in aqueous medium and its synergistic and specific adsorption for heavy metals from wastewater. Chemical Engineering Journal 360, 1486-1497.

Cheng, T.W., Lee, M.L., Ko, M.S., Ueng, T.H., Yang, S.F., 2012. The heavy metal adsorption characteristic on metakaolin-based geopolymer. Applied Clay Science 56, 90-96.

Choi, K., Lee, S., Park, J.O., Park, J-A., Cho, S-H., Lee, S.Y., Lee, J.H., Jae-Woo Choi, J.W., 2018. Chromium removal from aqueous solution by a PEI-silica nanocomposite. Scientific Reports 8, 1438.

Ebadi, M., H. Shagholani, H., Jahangiri, H., 2016. High Efficient Nanocomposite for Removal of Heavy Metals ($Hg^{2+}$ and $Pb^{2+}$) from Aqueous Solution. Journal of Nanostructures 6, 23-27.

El-Sadaawy, M., Abdelwahab, O., 2014. Adsorptive removal of nickel from aqueous solutions by activated carbons from doum seed (Hyphaenethebacia) boat. Alexandria Engineering Journal 53, 399-408.

Esmat, M., Farghali, A.A., Khder, M.H., El-Sherbiny, I.M., 2017. Alginate-based nanocomposites for efficient removal of heavy metal ions. International Journal of Biological Macromolecules 102, 272-283.

Farhan, A. M., Aldujaili, A.H., Awwad, A.M., 2013. Equilibrium and kinetics studies of cadmium and lead ions biosorption onto *Ficus carcia* leaves. International Journal of Industrial Chemistry 4, 24.

Farhan, A.M., Salem, N.S., Ahmad, A.L., Awwad, A.M., 2012. Kinetic, equilibrium and thermodynamic studies of the biosorption of heavy metals by *Ceratonia siliqua* bark. American Journal of Chemistry 2, 335-342.

Freundlich, HMF, Hellen, W., 1939. The adsorption of cis- and trans-azobenzene. Journal of the American Chemical Society 61, 2228-2230.

Gaikwad, R.W., Sapka, R.S., Sapka, V.S., 2010. Removal of copper ions from acid mine drainage wastewater using ion exchange technique: Factorial design analysis. Journal of Water Resource and Protection 2, 984-989.

Godiya, C.B., Cheng, X., Deng, G., Li, D., Lu, X., 2019a. Silk fibroin/polyethylenimine functional hydrogel for metal ion adsorption and upcycling utilization. Journal of Environmental Chemical Engineering 7, 102806.

Godiya, C.B., Cheng, X., Li, D., Chen, Z., Lu, X., 2019b. Carboxymethyl cellulose/polyacrylamide composite hydrogel for cascaded treatment/reuse of heavy metal ions in wastewater. Journal of Hazardous Materials 364, 28-38.

Güzel, F., Yakut, H., Topal, G., 2008. Determination of kinetic and equilibrium parameters of the batch adsorption of Mn(II), Co(II), Ni(II), and Cu(II) from aqueous solution by black carrot (*Daucua carota* L.) residues. Journal of Hazardous Materials 153, 1275-1287.

Ho, Y.S., 2006. Review of second-order models for adsorption systems. Journal of Hazardous Materials 136, 681-689.

Hu, Y., Zhu, J., Liu, Y., 2017. Removal of chromium(VI) from aqueous solutions by electrochemical reduction–precipitation. International Journal of Electrochemical Science 12, 11387–11396.

Ibrahim, B.M., Fakhre, N.A., 2019. Crown ether modification of starch for adsorption of heavy metals from synthetic wastewater. International Journal of Biological Macromolecules 123, 70-80.

Jiang, C., Wang, X., Wang, G., Hao, C., Li, X., Li, T., 2019. Adsorption performance of a polysaccharide composite hydrogel based on crosslinked glucan/chitosan for heavy metal ions. Composites Part B: Engineering 169, 45-54.

Jiang, M-Q., Jin, X-Y., Lu, X-Q., Chen, Z-l., 2010. Adsorption of Pb(II), Cd(II), Ni(II) and Cu(II) onto natural kaolinite clay. Desalination 252, 33-39.

Kamel, M.M., Ibrahm, M.A., Ismael, A.M., El-Motaleeb, M.A., 2004. Adsorption of some heavy metal ions from aqueous soliutions by using kaolinite clay. Assiut University Bulletin for Environmental Researches 7, 101-110.

Kausar, A., Iqbal, M., Javed, A., Aftab, K., Nazli, Z.-i.-H., Bhatti, H.N., Nouren, S., 2018a. Dyes adsorption using clay and modified clay: A review. Journal of Molecular Liquids 256, 395-407.

Kausar, A., MacKinnon, G., Alharthi, A., Hargreaves, J., Bhatti, H.N., Iqbal, M., 2018b. A green approach for the removal of Sr(II) from aqueous media: Kinetics, isotherms and thermodynamic studies. Journal of Molecular Liquids 257, 164-172.

Khera, R.A., Iqbal, M., Jabeen, S., Abbas, M., Nazir, A., Nisar, J., Ghaffar, A., Shar, G.A., Tahir, M.A., 2019. Adsorption efficiency of Pitpapra biomass under single and binary metal systems. Surfaces and Interfaces 14, 138-145.

Kounou, G.N., Nsami, J.N., Belibi, D.P.B., Kouotou, Tagne, G.M., Joh, D.D.D., Mbadcam, J. K., 2015. Adsorption of Zn (II) ions from aqueous solution onto kaolinite and metakaolinite. Der Pharma Chemica 7, 51-58.

Kuchekar, S., Gaikwad, V., Sonawane, D.V., 2014. Removal of hexavalent chromium from industrial effluents by natural ion exchanger. Indian Journal of Chemical Technology 21, 338-344.

Kumrić, K.R., Đukić, A.B., Trtić-Petrović, T.M., Vukelić, N.S., Stojanović, Z., Novaković, J.D.G., Matović. L.L., 2013. Simultaneous removal of divalent heavy metals from aqueous solutions using raw and mechanochemically treated interstratified montmorillonite/kaolinite clay. Industrial & Engineering Chemistry Research 52, 7930–7939.

Langmuir, I., 1918. Adsorption of gases on plain surfaces of glass, mica and platinum. Journal of the American Chemical Society 40, 1361-1403.

Liang, F-B., Song, Y-L., Huang, C-P., Y-X., Li, Y-X., and Chen, B.H., 2013. Synthesis of novel lignin-based ion-exchange resin and its utilization in heavy metals removal. Industrial & Engineering Chemistry Research 52, 1267–1274

Liu, W., Ni, J., Yin, X., 2014. Synergy of photocatalysis and adsorption for simultaneous removal of Cr(VI) and Cr(III) with $TiO_2$ and titanate nanotubes. Water Research 53, 12–25.

Matłok, M., Petrus, R., Warchoł, J.K., 2015. Equilibrium study of heavy metals adsorption on kaolin. Industrial & Engineering Chemistry Research 54, 6975–6984.

Mellah A. and Chegrouche, S.,1997. The removal of zinc from aqueous solutions by natural bentonite. Water Research 3, 621-629

Meroufel, B., Benali, O., Benyahia, M., Zenasni, M.A., Merlin, A., George B., 2013. Removal of Zn (II) from aqueous solution onto kaolin by batch design. Journal of Water Resource and Protection 5, 669-680.

Minas, F., Chandravanshi, B.S., SeyoumLeta, S., 2017. Chemical precipitation method for chromium removal and its recovery from tannery wastewater in Ethiopia.Chemical composition of food and environmental samples. Chemistry International 3, 291-305

Mousavi, S.V., Bozorgian, A., Mokhtari, N., Gabris, M.A., Rashidi Nodeh, H., Wan Ibrahim, W.A., 2019. A novel cyanopropylsilane-functionalized titanium oxide magnetic nanoparticle for the adsorption of nickel and lead ions from industrial wastewater: Equilibrium, kinetic and thermodynamic studies. Microchemical Journal 145, 914-920.

Nadeem, R., Manzoor, Q., Iqbal, M., Nisar, J., 2016. Biosorption of Pb(II) onto immobilized and native Mangifera indica waste biomass. Journal of Industrial and Engineering Chemistry 35, 185-194.

Onundi, Y.B., Mamu, A.A., Al Khatib, M.F., and Ahmed, Y.M., 2010. Adsorption of copper, nickel and lead ions from synthetic semiconduct or industrial wastewater by palm shell activated carbon. International Journal of Environmental Science and Technology 7, 751-758.

Orhan, Y., Buyukgungör, H., 1993. The removal of heavy metals by using agricultural waste. Water Science and Technology 28, 247-255.

Pang, M., Kano, N., Imaizumi, H., 2015. Adsorption of chromium (VI) from aqueous solution using zeolite/chitosan hybrid composite. Journal of Chemistry and Chemical Engineering 9, 433-441.

Revathi, M., saravanan, M., Chiya, A.B., Velan, M., 2012. Removal of copper, nickel and zinc ions from electroplating rinse water, Clean-Soil, Air, Water 40, 66-79.

Salem, N.M., Awwad, A.M., 2014. Biosorption of Ni(II) from electroplating wastewater by modified (*Eriobotrya japonica*) loquat bark. Journal of Saudi Chemical Society 18, 379–386.

Sandoval, O.G.M., Orozco, A.E.L., Valenzuela, S., Trujillo, G.C.D., 2019. Modified amorphous silica from a geothermal central as a metal adsorption agent for the regeneration of wastewater. Water Resources and Industry 21, 100105.

Sdiri, A., Higashi T., Jamoussi F., 2014. Adsorption of copper and zinc onto natural clay in single and binary systems. International Journal of Environmental Science and Technology 11, 1081-1092.

Shao-Feng, N., Yong, L., Xu Xin-Hua, X., 2005. Removal of hexavalent chromium from aqueous solution by iron nanoparticles. Journal of Zhejiang University Science B 6, 1022-1027.

Sitko, R., Turek, E., Zawisza, B., Malicka, E., Talik, E., Heimann, J., Gagor, A., Feist, B., Wrzalik, R., 2013. Adsorption of divalent metal ions from aqueous solutions using graphene oxide. Dalton Transactions 42, 5682-5689.

Sitko, R., Turek, E., Zawisza, B., Malicka, E., Talik, E., Heimann, J., Gagor, A., Feist, B., Wrzalik, R., 2013. Adsorption of divalent metal ions from aqueous solutions using graphene oxide. Dalton Transactions 42, 5682-5689.

Taseidifar, M., Makavipour, F., Pashley, R.M., Rahman, A.F., 2017. Removal of heavy metal ions from water using ion flotation. Environmental Technology & Innovation 8, 182-190.

Tripathi, A. and Dwivedi, A.K., 2012. Studies on recovery of chromium from tannery wastewater by reverse osmosis. Journal of Industrial Pollution Control 28, 29-34.

Un, U.T., Ocal, S.F.,2015. Removal of heavy metals (Cd, Cu, Ni) by electrocoagulation. International Journal of Environmental Science and Development 6, 425-428.

US Environmental Protection Agency (US EPA), 2004. Guidelines for Water Reuse, Office of Wastewater Management Office of Water, Washington DC, 2004, EPA/R04/108.

Veli, S., Alyuz, B., 2007. Adsorption of copper and zinc from aqueous solutions by using natural clay. Journal of Hazardous Materials 149, 226–233.

Verma, S.K., Khandegar, V., Anil K Saroha, A.K., 2013. Removal of chromium from electroplating industry effluent using electrocoagulation. Journal of Hazardous, Toxic, and Radioactive Waste 17, 2. DOI: 10.1061/(ASCE)HZ.2153-5515.0000170.

Wahyuni, E.T., Aprilita, N.H., Hatimah, H., Wulandari, A.M., Mudasir, M., 2015. Removal of toxic metal ions in water by photocatalytic method, American Chemical Science Journal 5, 194-201.

World Health Organization (WHO), 2008. Guidelines for Drinking-Water Quality, Incorporating 1st and 2nd Addenda, 3rd Edition, Vol. 1, Recommendations, Geneva.

Yavuz, O., Altunkaynak, Y., Guzel, F., 2003. Removal of copper, nickel, cobalt and manganese from aqueous solution by kaolinite. Water Research 37, 948-952.

Zafar, M.N., Dar, Q., Nawaz, F., Zafar, M.N., Iqbal, M., Nazar, M.F., 2018. Effective adsorptive removal of azo dyes over spherical ZnO nanoparticles. Journal of Materials Research and Technology.

Zhan, W., Xu, C., Qian,G., Huang, G., Tang, X., Lin, B., 2018. Adsorption of Cu(II), Zn(II), and Pb(II) from aqueous single and binary metal solutions by regenerated cellulose and sodium alginate chemically modified with polyethyleneimine. RSC Advances 8, 18723-18733.

Zhang, X., and Wang, X., 2015. Adsorption and desorption of nickel (II) Ions from aqueous solution by a lignocellulose/montmorillonite nanocomposite, Plos One 10, e0117077.

Zhang, X., Hao, Y., Wang, X., Z. Chen, Z., 2017. Rapid removal of zinc(II) from aqueous solutions using a mesoporous activated carbon prepared from agricultural waste. Materials (Basel) 10, E1002.

Zhao, M., Wang, S., Wang, H., Qin, P., Yang, D., Sun, Y., Kong, F., 2019. Application of sodium titanate nanofibers as constructed wetland fillers for efficient removal of heavy metal ions from wastewater. Environmental Pollution 248, 938-946.

Visit us at: http://bosaljournals.com/chemint/
Submissions are accepted at: editorci@bosaljournals.com